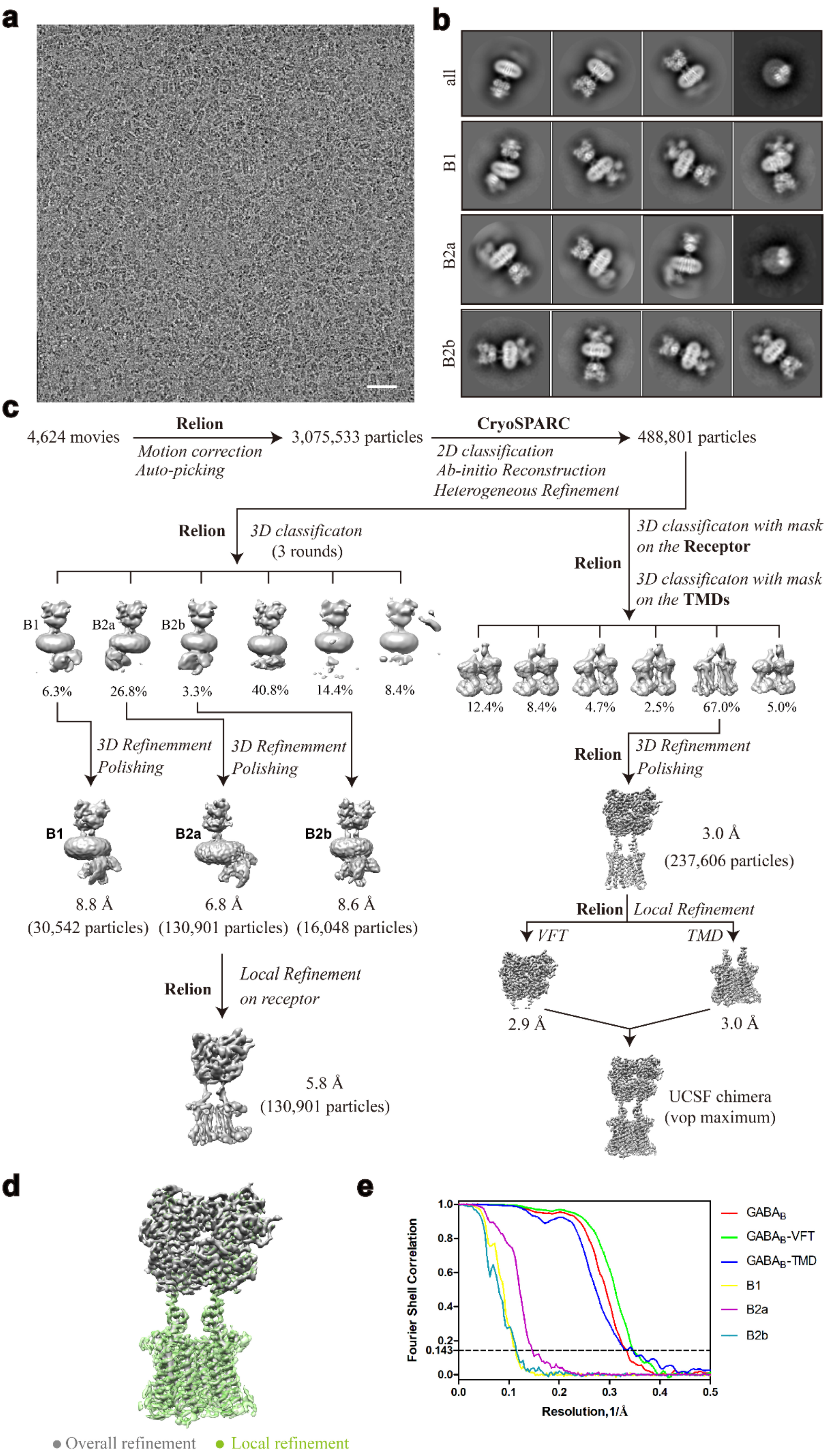a
b
all
B1
B2a
B2b
c
4,624 movies
Relion
Motion correction
Auto-picking
3,075,533 particles
CryoSPARC
2D classification
Ab-initio Reconstruction
Heterogeneous Refinement
488,801 particles
Relion
3D classificaton
(3 rounds)
B1
B2a
B2b
6.3%
26.8%
3.3%
40.8%
14.4%
8.4%
3D Refinemment
Polishing
3D Refinemment
Polishing
B1
B2a
B2b
8.8 Å
(30,542 particles)
6.8 Å
(130,901 particles)
8.6 Å
(16,048 particles)
Relion
Local Refinement
on receptor
5.8 Å
(130,901 particles)
Relion
3D classificaton with mask
on the Receptor
3D classificaton with mask
on the TMDs
12.4%
8.4%
4.7%
2.5%
67.0%
5.0%
Relion
3D Refinemment
Polishing
3.0 Å
(237,606 particles)
Relion
Local Refinement
VFT
TMD
2.9 Å
3.0 Å
UCSF chimera
(vop maximum)
d
● Overall refinement
● Local refinement
e
Fourier Shell Correlation
1.0
0.8
0.6
0.4
0.2
0.143
0.0
0.0
0.1
0.2
0.3
0.4
0.5
Resolution,1/Å
GABA$_B$
GABA$_B$-VFT
GABA$_B$-TMD
B1
B2a
B2b

Supplementary information, Figure S3 Single-particle reconstruction of the agonist/PAM-bound GABA$_B$–G$_{i1}$ complex. a Representative cryo-EM micrograph of the GABA$_B$–G$_{i1}$ complex (scale bar: 30 nm). **b** Representative two-dimensional class averages of the overall refined GABA$_B$ receptor (all) and the GABA$_B$–G$_{i1}$ complex in B1, B2a and B2b states, respectively (scale bar: 5 nm). **c** Flow chart of cryo-EM data processing. Details are described in method section. **d** Comparison of the overall refined map and the locally refined composite map. The locally refined composite map shows a substantial improvement for the TM density and exhibits almost the same conformation with the overall refined map. **e** Gold-standard Fourier shell correlation curves of overall refined receptor, the locally refined VFT and TMD and the refined GABA$_B$-G$_{i1}$ complex in B1, B2a, B2b states.